Materials Research Proceedings **24** (2022) 254-261 https://doi.org/10.21741/9781644902059-37

Analysis of Pressure Distribution in Non-Contacting Impulse Gas Face Seals

BŁASIAK Slawomir[1,a*] and TAKOSOGLU Jakub[1,b]

[1]Kielce University of Technology, Faculty of Mechatronics and Mechanical Engineering, Al. 1000-lecia Państwa Polskiego 7, 25-314 Kielce, Poland

[a]sblasiak@tu.kielce.pl, [b]qba@tu.kielce.pl

Keywords: Impulse Gas Face Seals, Dynamic, Reynolds Equation, Numerical Method

Abstract. Strict norms regarding the emission of harmful substances into the natural environment impose stringent requirements on engineers designing sealing units, especially when designing new mechanical seals. This especially concerns mechanical non-contacting seals with various surface layer modifications. Complex mathematical models that enable analyzing complex physical phenomena are developed to support the designing works. The presented paper includes specification of the impulse gas face seals mathematical model which takes into consideration the non-linear Reynolds equation. The mathematical model was solved based on the author's computer program developed in the C++ language, thereby enabling a series of numerical tests and analyses on the phenomena taking place in the radial clearance during the seal's operation. The paper also includes the final conclusions and a series of features specific for the subject impulse gas face seals.

Introduction

Mechanical seals were firmly established as structural elements of sealing units. In recent years, the literature on sealing technology featured a series of papers on non-contacting face seals. It is important to note that such seals are used in virtually all industry branches and operate in extremely different operating and environmental conditions. They are used in rotor machines, including compressors, high-speed pumps, mixers, etc. They play a crucial role in separating the sealed working mediums from the external environment. Many variants of non-contacting face seals that enabled achieving the assumed goal to a lesser or higher degree were developed over the years. The recurring problem in virtually all designs is to maintain a stable separation clearance between work rings. In the case of non-contacting gas face seals, one of the methods that enable maintaining a stable medium layer is to introduce various geometric modifications (micro-structures) to the work rings' tracks. These can include radial or spiral grooves [1,2] or face surface texturing [3]. Introducing changes to the sealing rings' face surfaces causes changes in the fluid film's dynamic properties. Ensuring balance between the forces acting on the ring system allows for maintaining a stable medium layer and prevents contact between the rings during operation. The results of testing on the impact of geometric changes in the applied face surface modifications on the fluid film's dynamic properties are included in [4–10], among others.

In papers [11–15] the authors present the results of numerical analyses of a complex mathematical model encompassing the ring vibration dynamics' equations and the non-linear Reynolds equation for a compressible medium. The calculation of forces and hydrodynamic moments requires solving the Reynolds equation and designating the pressure distribution in the fluid film. In the discussed papers, the two-dimensional Reynolds equation is solved with the use of numerical methods.

Materials Research Proceedings **24** (2022) 254-261 https://doi.org/10.21741/9781644902059-37

The most common methods used include: Finite Volume Method (FVM) [16,17], Finite Element Method (FEM) [18], while the Finite Difference Method is used less often. The correct designation of the pressure distribution, especially in a clearance with complex topography, determines the accuracy of the obtained forces and (hydro-)gaso-dynamic moments obtained.

This paper presents model testing of little-known non-contacting impulse gas face seals. It includes a mathematical model solved using numerical methods and procedures collected in the author's computer program. The paper also includes results of tests mainly concerning pressure changes in the radial clearance at various stages of operation of non-contacting impulse gas face seals.

Subject of Testing

The specificity of non-contacting gas face seals assumes their operation with a certain minimum leakage. A feature specific to non-contacting seals is that they maintain a stable clearance restricting the leak between the interoperating face surfaces of the rings.

Based on [19–23] Fig. 1 presents a drawing of a non-contacting impulse gas face seal.

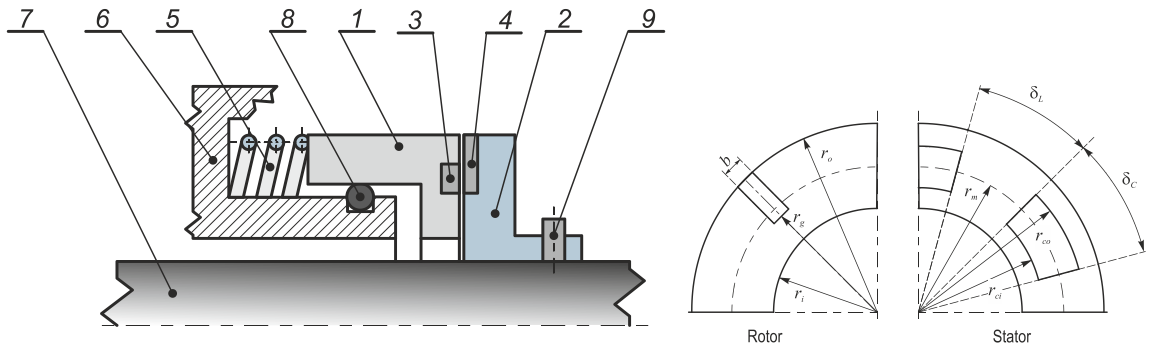

***Fig. 1**. Cross section scheme of a non-contacting impulse gas face seal; 1 – stator, 2 – rotor, 3 – chamber, 4 – parallel groove, 5 – spring, 6 – casing, 7 – shaft, 8 – O-ring, 9 – steady pin.*

This seal, similarly to traditional non-contacting gas face seals, consists of two rings. The stator (1) is embedded flexibly in the casing and its face surface features peripherally closed chambers (3). On the other hand, the rotor (2) turns along with the rotor machine's shaft (6) and its face surface includes open radial grooves (4). The grooves are facing the process side (gland) space filled with the sealed medium with a set pressure P_o. The operating principle for the impulse gas face seal was provided in the papers of the creators of such seals [24].

During operation, the sealed medium quickly flows (is injected) from the gland to the aforementioned chamber when the groove (4) overlaps with the chamber (3). The chamber features a rapid pressure increase at that time. When the groove passes a peripheral section equal to the chamber's length, the pressure in the chamber decreases due to the medium's leakage via the outer peripheral area. The pressure decrease in the chamber lasts until the next medium injection (pressure impulse).

The presented mode of operation of non-contacting impulse gas face seals ensures the maintenance of a continuity of the gas film of a low height (several micrometers) and prevents contact between the work rings during the device's operation.

Mathematical Model

It can be stated that the mathematical model for the non-contacting impulse gas face seal is widely known. The subject literature (e.g. [25]) describes it as a discrete and continuous system of differential equations, e.g. equations describing the vibration of a ring mounted flexibly in a casing,

equations describing the film fluid's motion and equations describing the stream continuity (mass conservation equation). By applying widely known simplifying assumptions, the motion equation and continuity equation were brought down to a single equation that described the pressure distribution in the radial clearance, i.e. the so-called Reynolds equation [26].

$$\vec{\nabla}\left[p h^3 \vec{\nabla} p - 6\mu\omega r\, p h \vec{e}_\theta \right] = 12\mu \frac{\partial (p h)}{\partial t} \tag{1}$$

It is possible to designate the pressure distribution when adopting the following boundary conditions and periodicity condition:

$$p(r,\theta)\big|_{r=r_i} = p_i\,;\ p(r,\theta)\big|_{r=r_o} = p_o\,;\ p(r,\theta)\big|_{\theta=0} = p(r,\theta)\big|_{\theta=2\pi} \tag{2}$$

The Reynolds equation (1) is a non-linear equation. It specifies pressure changes in the radial clearance for compressible media. When conducting a dependency analysis (1), it can be stated that the pressure distribution in the clearance depends mainly on the function describing the radial clearance's height. With the assumption of a parallel position of the interoperating rings, the distance of any point located on the ring surfaces in regards to the beginning of the inertial coordinates system is presented as a dependency for the stator and rotor, respectively:

$$h^s = -h_c(r,\theta) \tag{3}$$

$$h^r = h_o + h_g(t,r,\theta) \tag{4}$$

The formula describing the simplified radial clearance height function was obtained by subtracting equation (4) from (3).

$$h(t,r,\theta) = h^r - h^s = h_o + h_g(t,r,\theta) + h_c(r,\theta) \tag{5}$$

The nominal radial clearance height h_o derives from the balance of forces acting on the work ring system and is determined during the designing of the given non-contacting impulse gas face seal. In the discussed example, the calculations featured the assumption that $h_o = 6\,\mu m$. Special attention must be paid to the surface functions h_c and h_g that describe the geometry of the chambers and grooves on the face surfaces of the stator and rotor, respectively. The function $h_g(t,r,\theta)$ also takes into account the rotational motion of the rotor along with the radial grooves (provided on the rotor's face surface) with the angular velocity ω.

Numerical Solution of the Reynolds Equation

In the presented paper, the equation (1) was solved by using the numerical method specified in the literature in more detail, i.e. the Finite Volume Method. The method is often used in numerical solutions of differential equations with partial derivatives, especially in the case of notions concerning convection and diffusion. The figure below presents a scheme for the FVM calculation grid.

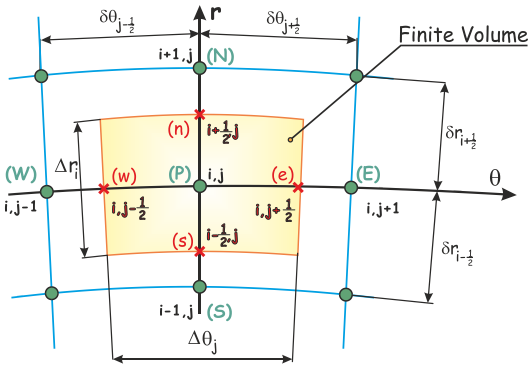

Fig. 2. *Finite volume grid scheme.*

Virtually two Reynolds equations were solved in the presented FVM calculation algorithm. The first case concerned the designation of the steady state pressure distribution and the calculations did not feature the derivative $\frac{\partial p}{\partial t}$.

$$\int_s^n\int_w^e \frac{\partial}{\partial r}\left(p h^3 r \frac{\partial p}{\partial r}\right) dr\, d\theta + \int_s^n\int_w^e \frac{\partial}{\partial \theta}\left(\frac{p h^3}{r}\frac{\partial p}{\partial \theta} - 6\mu\omega r\, p h\right) dr\, d\theta = 12\int_s^n\int_w^e \mu r\, p \frac{\partial h}{\partial t} dr\, d\theta \tag{6}$$

In the second case, the complete Reynolds equation (1) was solved:

$$12\int_s^n\int_w^e \mu r h \frac{\partial p}{\partial t} dr\, d\theta = \int_s^n\int_w^e \frac{\partial}{\partial r}\left(p h^3 r \frac{\partial p}{\partial r}\right) dr\, d\theta +$$

$$+\int_s^n\int_w^e \frac{\partial}{\partial \theta}\left(\frac{p h^3}{r}\frac{\partial p}{\partial \theta} - 6\mu\omega r\, p h\right) dr\, d\theta - 12\int_s^n\int_w^e \mu r\, p \frac{\partial h}{\partial t} dr\, d\theta . \tag{7}$$

The following dependency was obtained by integrating particular components of the equation (6) on the elementary finite volume:

$$\left(A_N + A_S + A_E + A_W + F_e - F_w + \bar{S}\right) p_P = A_N p_N + A_S p_S + A_E p_E + A_W p_W \tag{8}$$

where:

$$A_N = D_n \quad A_S = D_s \tag{9}$$

$$A_E = D_e + \max(0, -F_e) \quad A_W = D_w + \max(F_w, 0) \tag{10}$$

The elements present in the aforementioned components depend on the pressure in the *N,S,W,E* and *P* grid nodes and refer to convection and diffusion on each finite volume surface.

$$D_n = \left(\frac{p h^3 r \Delta\theta}{\Delta r}\right)_n ;\ D_s = \left(\frac{p h^3 r \Delta\theta}{\Delta r}\right)_s ;\ D_e = \left(\frac{p h^3 \Delta r}{r \Delta\theta}\right)_e ;\ D_w = \left(\frac{p h^3 \Delta r}{r \Delta\theta}\right)_w .$$

$$F_e = \left(6\mu\omega r h \Delta r\right)_e ,. F_w = \left(6\mu\omega r h \Delta r\right)_w ., \overline{S} = \left(12\mu r \frac{\partial h}{\partial t}\Delta r \Delta\theta\right)$$

The main deficiency of the presented central differential scheme (equation (8)) is its dependency on the direction of flow. The upwind differential scheme, the general form of which was written as dependency (10), was introduced to improve the solution's stability.

$$\left(12\mu r h \Delta r \Delta\theta\right)\frac{\partial p}{\partial t} = \left(A_N + A_S + A_E + A_W + F_e - F_w + \overline{S}\right)p_P - A_N p_N - A_S p_S - A_E p_E - A_W p_W \tag{11}$$

In the case of the complete non-stationary Reynolds equation (7) (encompassing the pressure derivative over time), it will assume a discretized form as in (11). In the case of the Finite Volume Method, the boundary conditions written with dependency (2) can be easily implemented into the calculations.

Results and Discussion

The solution of the developed numerical model required the introduction of a series of parameters that describe the geometry and working conditions of the impulse gas face seals.

In the case of the impulse face seals, the numerical designation of pressure distribution in the fluid film can cause some problems. As opposed to traditional gas face seals which feature modifications to the sealing rings' tracks in the form of geometric structures (micro-channels, texturing, etc.) applicable only to the (e.g.) stator's surface, the impulse gas face seals also require modeling of the grooves located on the rotor's face surface and move along with the rotor. This means that the aforementioned grooves must move continuously and periodically on the generated calculation grid throughout the entire computer simulation's duration. The results obtained based on the developed numerical algorithm and the author's computer program are presented below. The pressure value was designated at the checkpoint placed on the ring's circumference, in the central part of the chamber located on the stator's surface. The parameters presented in Table 1 were used in the numerical calculations.

It was assumed that the nominal radial clearance height amounted to $h_o = 6\cdot 10^{-6}\left(m\right)$, whereas the depth of the chambers and grooves amounted to $h_g = h_c = 6\cdot 10^{-6}\left(m\right)$.

Table 1. *Gas face seal geometry- and performance-related parameters.*

Parameter	Value	Parameter	Value
Shaft angular velocity	$\omega = 2094\left[rad/s\right]$	Inner radius	$r_i = 0.048\left[m\right]$
Gas viscosity	$\mu = 1.8\left(10^{-5}\right)\left[Pa\,s\right]$	Outer radius	$r_o = 0.060\left[m\right]$
Design clearance	$h_o = 6\left(10^{-6}\right)\left[m\right]$	Chamber inner radius	$r_{ci} = r_m$
Groove depth	$h_g = 6\left(10^{-6}\right)\left[m\right]$	Chamber outer radius	$r_{co} = 0.8\cdot r_o$
Chamber depth	$h_c = 6\left(10^{-6}\right)\left[m\right]$	Groove radius	$r_g = r_m = 0.5\left(r_i + r_o\right)$
Pressure on the inner radius	$p_i = 1\left(10^{5}\right)\left[Pa\right]$	Number of grooves	$n_g = 3$
Pressure on the outer radius	$p_o = 2\left(10^{5}\right)\left[Pa\right]$	Number of chambers	$n_c = 6$

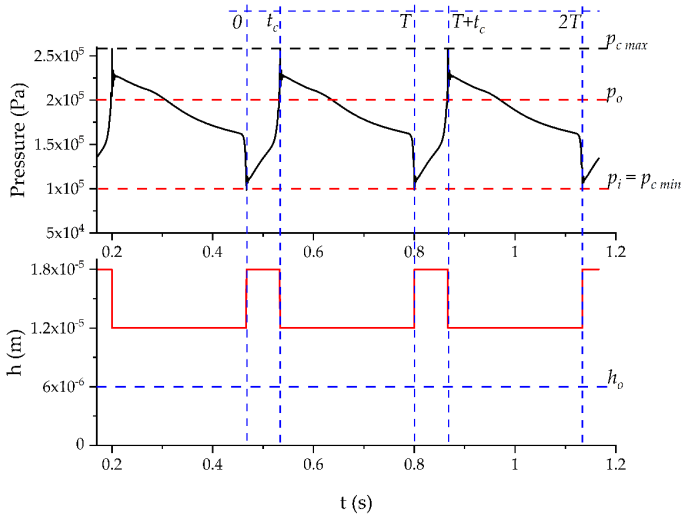

Fig. 3. *Pressure changes in a single chamber*

When analyzing the pressure changes in a single chamber (Fig. 3), it is possible to note that an impulse pressure increase of up to $2.25 \cdot 10^5 (Pa)$ takes place at the instance of time t_c. It is also necessary to note the phenomenon related to the pressure instability of $2.5 \cdot 10^5 (Pa)$. When the groove passes the chamber area, the chamber features a pressure drop of up to $p_{c\min}$. For the adopted sealing ring geometry, it was noted that for the nominal radial clearance height of $h_o = 6 \cdot 10^{-6} (m)$, the pressure value is $p_{c\min} \approx\sim 1 \cdot 10^5 (Pa)$.

In the subject literature, non-contacting impulse gas face seals are often described as semi-active or self-adjusting seals [22, 24]. In the discussed structural solution, the self-adjustment of the radial clearance height is generated through the selection (during the designing phase) of the geometric parameters of the modifications applied to the rings' face surfaces. The expected radial clearance height is obtained by "adjusting" the hydrodynamic force (opening force) generated in the fluid film. In terms of structural assumptions, the perfect operation of a pair of sealing rings should feature the maintenance of the radial clearance height of ($h / h_o \approx 1$), whereas the vibration amplitude should be as small as possible. Maintaining this regime also ensures minimum leakage. In addition, it reduced the probability of contact between the rings, thereby preventing their excessive wear.

The pressure distribution in the radial clearance of non-contacting impulse gas face seals is presented graphically for the parameters given in Table 1.

a) *b)*

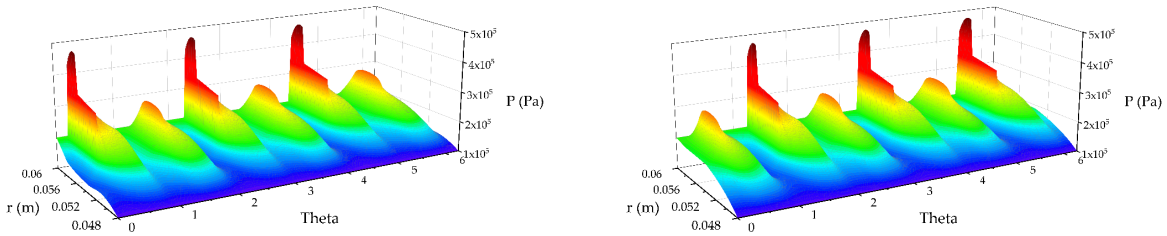

Fig. 4. *Pressure changes in a single chamber*

Fig. 4 presents pressure distributions in the radial clearance in subsequent phases of pressure operation. When analyzing the presented results, it is possible to note the groove motion along the

counter ring's track which causes an increase in the medium's pressure along the entire groove length.

Summary

This paper presents the structure, working principle and model testing of little-known non-contacting impulse gas face seals. It also includes the development of a mathematical model as well as numerical calculations featuring the solution of the non-linear Reynolds equation. The obtained results are presented in the form of plots featuring pressure distributions in the radial clearance during the discussed seal's various operation cycles. It can be stated that the reliability and durability of any non-contacting seal, not only the impulse gas face seals, depends on the radial clearance height occurring between the surfaces of a pair of work rings. The above deliberations feature clear advantages of the discussed impulse gas face seals, including: effective heat dissipation, reversibility in regards to the rotation directions, substantial reduction of dimensions when compared to conventional mechanical face seals. The main disadvantage is the presence of moving feed grooves made on the rotor, which pose the risk of clogging. The computer program developed by the author can be a good tool for supporting the designing of new impulse gas face seals. It can also be useful in the selection of adequate geometric parameters of chambers and grooves enabling the achievement of the set operating conditions.

References

[1] R.A. Shellef, R.P. Johnson. A Bi-Directional Gas Face Seal, Tribology Trans. 35 (1992) 53–58. https://doi.org/10.1080/10402009208982088.

[2] N. Zirkelback. Parametric study of spiral groove gas face seals, Tribol. Trans. 43 (2000) 337-343. https://doi.org/10.1080/10402000008982349.

[3] Y. Feldman, Y. Kligerman, I. Etsion. A Hydrostatic Laser Surface Textured Gas Seal, Tribology Lett. 22 (2006) 21-28. https://doi.org/10.1007/s11249-006-9066-z.

[4] S. Blasiak. Influence of Thermoelastic Phenomena on the Energy Conservation in Non-Contacting Face Seals, Energies 13 (2020) art. 5283. https://doi.org/10.3390/en13205283

[5] S. Blasiak. Heat Transfer Analysis for Non-Contacting Mechanical Face Seals Using the Variable-Order Derivative Approach, Energies 14 (2021) art. 5512. https://doi.org/10.3390/en14175512

[6] I. Green. A Transient Dynamic Analysis of Mechanical Seals Including Asperity Contact and Face Deformation, Tribol. Trans. 45 (2002) 284–293. https://doi.org/10.1080/10402000208982551

[7] B. Wang. Numerical Analysis of a Spiral-groove Dry-gas Seal Considering Micro-scale Effects, Chinese Journal of Mechanical Engineering 24 (2011) 146 https://doi.org/10.3901/CJME.2011.01.146

[8] B.A. Miller, I. Green. Semi-Analytical Dynamic Analysis of Spiral-Grooved Mechanical Gas Face Seals, Journal of Tribology 125 (2003) 403–413. https://doi.org/10.1115/1.1510876

[9] B.A. Miller, I. Green. Numerical Formulation for the Dynamic Analysis of Spiral-Grooved Gas Face Seals, Journal of Tribology 123 (2001) 395–403. https://doi.org/10.1115/1.1308015

[10] B.A. Miller, I. Green. Numerical Techniques for Computing Rotordynamic Properties of Mechanical Gas Face Seals, Journal of Tribology 124 (2002) 755–761. https://doi.org/10.1115/1.1467635

[11] I. Green, R.M. Barnsby. A Simultaneous Numerical Solution for the Lubrication and Dynamic Stability of Noncontacting Gas Face Seals, Journal of Tribology 123 (2001) 388–394.

https://doi.org/10.1115/1.1308020
[12] S. Hu, W. Huang, X. Liu, Y. Wang. Stability and tracking analysis of gas face seals under low-parameter conditions considering slip flow, Journal of Vibroengineering 19 (2017) 2126–2141. https://doi.org/10.21595/jve.2016.17111
[13] S. Blasiak. An analytical approach to heat transfer and thermal distortions in non-contacting face seals, International Journal of Heat and Mass Transfer 81 (2015) 90–102. https://doi.org/10.1016/j.ijheatmasstransfer.2014.10.011
[14] W. Xu, J. Yang. Spiral-grooved gas face seal for steam turbine shroud tip leakage reduction: Performance and feasibility analysis, Tribology International 98 (2016) 242–252. https://doi.org/10.1016/j.triboint.2016.02.035
[15] D. Bonneau, J. Huitric, B. Tournerie. Finite Element Analysis of Grooved Gas Thrust Bearings and Grooved Gas Face Seals, Journal of Tribology 115 (1993) 348-354. https://doi.org/10.1115/1.2921642
[16] S. Blasiak. Numerical modeling and analysis of the noncontacting impulse gas face seals, Proc. Institution of Mechanical Engineers Part J – Journal of Engineering Tribology 233 (2019) 1139-1153. https://doi.org/10.1177/1350650118817188
[17] S. Blasiak, A.V. Zahorulko. A parametric and dynamic analysis of non-contacting gas face seals with modified surfaces, Tribology International 94 (2016) 126–137. https://doi.org/10.1016/j.triboint.2015.08.014
[18] B. Ruan. Finite Element Analysis of the Spiral Groove Gas Face Seal at the Slow Speed and the Low Pressure Conditions – Slip Flow Consideration, Tribology Trans. 43 (2000) 411-418. https://doi.org/10.1080/10402000008982357
[19] A.V. Zahorulko. Theoretical and experimental investigations of face buffer impulse seals with discrete supplying, Eastern-European Journal of Enterprise Technologies 4 (2015) 45-52. https://doi.org/10.15587/1729-4061.2015.48298
[20] A. Zahorulko. Experimental investigation of mechanical properties of stuffing box packings, Sealing Technology 8 (2015) 7-13. https://doi.org/10.1016/S1350-4789(15)30244-0
[21] A. Zahorulko, D.V. Lisovenko, V. Martsynkovskyy. Development and investigation of face buffer impulse seal of centrifugal compressor, East.-Eur. J. Enterp. Technol. 1 (2016) 30-39. https://doi.org/10.15587/1729-4061.2016.59884
[22] V. Martsynkovskyy, A. Zahorulko, S. Gudkov, S. Mischenko. Analysis of Buffer Impulse Seal, Procedia Engineering 39 (2012) 43-50. https://doi.org/10.1016/j.proeng.2012.07.006
[23] V.A. Martsynkovskyy, S. Hudkov, C. Kundera. Influence of feeders on operating characteristics of the impulse seals, IOP Conf. Ser.: Mater. Sci. Eng. 233 (2017) art. 012033. https://doi.org/10.1088/1757-899X/233/1/012033
[24] V. Martsynkovskyy, C. Kundera, A. Khalizeva. The Calculation of Static Characteristics of Impulse Gas Seal, Applied Mechanics and Materials 630 (2014) 267-276. https://doi.org/10.4028/www.scientific.net/AMM.630.267
[25] B. Ruan. Numerical Modeling of Dynamic Sealing Behaviors of Spiral Groove Gas Face Seals, Journal of Tribology 124 (2002) 186-195. https://doi.org/10.1115/1.1398291
[26] I. Green, R.M. Barnsby. A Parametric Analysis of the Transient Forced Response of Noncontacting Coned-Face Gas Seals, Journal of Tribology 124 (2002) 151-157. https://doi.org/10.1115/1.1401015